Structure of the Active Site of Lignin Peroxidase Isozyme H2: Native Enzyme, Compound III, and Reduced Form†

R. Sinclair,‡ I. Yamazaki,‡ J. Bumpus,§ B. Brock,∥ C.-S. Chang,‡ A. Albo,⊥ and L. Powers*,‡

National Center for the Design of Molecular Function, Utah State University, Logan, Utah 84322-4630, College of Science, University of Notre Dame, Notre Dame, Indiana 46556, Oregon Graduate Institute of Science and Technology, 19600 Von Neumann Drive, Beaverton, Oregon 97006, and Biotechnology Center, Utah State University, Logan, Utah 84322-4430

Received June 13, 1991; Revised Manuscript Received March 3, 1992

ABSTRACT: The wood-degrading fungus *Phanerochaete chrysosporium* secretes a number of extracellular enzymes called lignin peroxidases which are involved in the degradation of both lignin and a number of persistent environmental pollutants. Lignin peroxidase isozyme H2, a glycosylated protein of approximately 40 kDa, contains a single heme. X-ray absorption spectroscopy (XAS) has been used to probe the local environment of the iron in the active site of resting enzyme, reduced enzyme, and compound III. For the native and reduced forms, respectively, the average Fe–pyrrole nitrogen distances are 2.055 and 2.02 Å (±0.015 Å); the Fe–proximal nitrogen distance is 1.93 and 1.91 Å (±0.02 Å) while the Fe–distal ligand distance is 2.17 and 2.10 Å (±0.03 Å). Although the results are not as well-defined, the active-site structure of compound III is largely 2.02 ± 0.015 Å for the average Fe–pyrrole nitrogen distance, 1.90 ± 0.02 for the Fe–proximal nitrogen, and 1.74 ± 0.03 Å for the Fe–distal ligand distance. The heme iron–pyrrole nitrogen distnce is more expanded in ligninase H2 than in other peroxidases. The possible significance of this is discussed in relation to other heme proteins.

The wood-degrading (white rot) fungus *Phanerochaete chrysosporium* (Burds) produces a number of extracellular enzymes in response to nutrient nitrogen or carbon depletion (Keyser et al., 1978; Jeffries et al., 1981). These enzymes fall into two classes called lignin peroxidases (ligninases) and manganese-dependent peroxidases. Although the role of the lignin peroxidases has been questioned both in lignin biodegradation (Sarkanen et al., 1991) and in xenobiotic degradation (Kohler et al., 1988), the lignin-degrading enzyme system of *P. chrysosporium* has also been demonstrated to play a significant role in these processes and appears to impart upon the fungus the ability to degrade lignin and to catalyze the initial oxidation of both lignin and lignin model compounds (Tien, 1987; Tien & Kirk, 1984; Gold et al., 1979). In addition, it has been demonstrated that the fungus is able to oxidize to carbon dioxide a number of persistent environmental pollutants (Bumpus et al., 1985; Bumpus & Aust, 1987a,b; Eaton, 1985; Arjmand & Sanderman, 1985; Bumpus & Brock, 1988; Mileski et al., 1988; Valli & Gold, 1991) and that the initial oxidation of several of these xenobiotic compounds is catalyzed by lignin peroxidase proteins (Bumpus & Brock, 1988; Mileski et al., 1988; Sanglard et al., 1986; Haemmerli et al., 1986; Hammel et al., 1986; Screiner et al., 1988; Hammel & Tardane, 1988; Valli & Gold, 1991). Farrel et al. (1989) have shown that at least 10 heme proteins are present in the extracellular fluid of ligninolytic cultures of *P. crysosporium*. These heme proteins have been designated H1 to H10, signifying the order in which they elute from anion-exchange columns during fast protein liquid chromatography. Six of these (H1, -2, -6, -7, -8, and -10) exhibit significant veratryl alcohol (VA) oxidation ability and were consequently grouped together as the lignin peroxidases. Of the remaining four, at least three demonstrated manganese-dependent vanillylacetone oxidizing ability and were therefore grouped as the manganese-dependent peroxidases. In other studies, Leisola et al. (1987) have presented evidence suggesting that up to 15 heme proteins may be present in the extracellular fluid of ligninolytic cultures of *P. chrysosporium*. Some biochemical properties of the lignin peroxidases have been determined. They all contain a single ferric protoporphyrin IX per molecule (Gold et al., 1984; Tien & Kirk, 1984) and have been shown to be N- and probably O-glycosylated. The molecular masses, determined by SDS–PAGE, range from 38 to 43 kilodaltons (kDa), and the proteins exhibit isoelectric points between 3.3 and 4.7. Antibodies raised against H2 or H8 are cross-reactive with other lignin peroxidases (Kirk et al., 1986), and the proteins have also been shown to be related by limited proteolytic analysis (Farrell et al., 1989). The DNA sequences of some isozymes have been determined (deBoer et al., 1987; Smith et al., 1988; Tien & Tu, 1987a,b; Pribnow et al., 1989; Godfrey et al., 1990; Zhang et al., 1991), which confirms the sequence similarities deduced above and predicts molecular masses of around 37 kDa for the unglycosylated proteins.

Under the stationary culture conditions used by Tien and Kirk (1984), lignin peroxidase H8 was the predominant isozyme produced and therefore was the first lignin peroxidase to be extensively characterized. Under our culture conditions, H2 is the predominant isozyme produced (Tuisel et al., 1990). Therefore, most of our studies were performed using this isozyme. This isozyme is probably identical to the H2 reported by Farrell et al. (1989). Although we will refer to it as H2, Farrell et al. (1989) additionally propose a nomenclature which would require that this protein be referred to as LiP2. H2 elutes from a Mono Q HR 5/5 column at approximately 0.18 molar sodium acetate. It has an SDS–PAGE determined molecular mass of 38 kDa and an isoelectric point of 4.4.

Analogous to other heme peroxidases (Yamazaki, 1974), the lignin peroxidase catalytic cycle begins with the reaction of resting enzyme (ferric, Fe^{3+}) with H_2O_2 to yield the ferryl iron (Fe^{4+}) porphyrin cation radical intermediate, compound

† Supported in part by NIEHS Superfund Grant ES 04922 and by Savannah River Laboratory Grant W 89329.

* To whom correspondence should be addressed.

‡ National Center for the Design of Molecular Function, Utah State University.

§ University of Notre Dame.

∥ Oregon Graduate Institute of Science and Technology.

⊥ Biotechnology Center, Utah State University.

0006-2960/92/0431-4892$03.00/0

I, which is 2 oxidizing equiv above the resting state. Compound I is reduced by one electron via a reducing substrate (such as veratryl alcohol) to yield the iron-oxo intermediate compound II. This is still ferryl iron (Fe^{4+}), but no longer has the porphyrin cation radical. Finally, a second single-electron reduction returns the enzyme to the resting state (Renganathan & Gold, 1986; Marquez et al., 1988). The electronic absorption spectrum of resting (ferric) enzyme is typical of heme peroxidases, showing a Soret absorption maximum at 408 nm and visible absorption bands at 504 and 636 nm. The ferric enzyme reacts with both cyanide and azide to form low-spin complexes (Dunford & Stillman, 1976; Gold et al., 1984). The ferrous complex is also typical of the heme peroxidases, exhibiting a significantly red-shifted Soret absorbance and the ability to form complexes with CO, NO, and O_2 (Andersson et al., 1985). The heme peroxidases are also able to form an additional intermediate, compound III, which is not involved in the normal catalytic cycle, but is of great interest from a structural and catalytic point of view. Some aspects of compound III of the lignin peroxidases are still unclear, and it is useful to review the relevant literature at this point. Four methods are described for the preparation of horseradish peroxidase (HRP) compound III (Yamazaki, 1974; Dunford & Stillman, 1976): (a) resting peroxidase reacted with excess H_2O_2; (b) reduction of resting peroxidase with sodium dithionite followed by addition of O_2; (c) addition of H_2O_2 to compound II; and (d) resting enzyme reacted directly with superoxide anion ($O_2^{\bullet-}$). The first reports of preparation of lignin peroxidase III (Renganathan & Gold, 1986) involved reaction of resting enzyme with 25 equiv of H_2O_2 at pH 6.0 and produced a sample having a Soret absorption at 420 nm and visible maxima at 540 and 578 nm. As with earlier studies on the peroxidases (Dunford & Stillman, 1976; Dunford, 1982), it proved impossible to distinguish this form as ferric-superoxide ($Fe^{3+}O_2^{\bullet-}$) or ferrous-oxy ($Fe^{2+}O_2$). At pH 3.0, addition of 20 equiv of H_2O_2 to the resting enzyme produced a spectrum similar to that described above (Wariishi & Gold, 1989; Cai & Tien, 1990; Wariishi et al., 1990). This species was reported to be easily inactivated, but was protected from inactivation by addition of VA. The compound III prepared for this study was observed to return to native enzyme in a single-step reaction, but the process was dependent on the presence of VA which was not consumed by the reaction. Addition of >30 equiv of H_2O_2 to enzyme at this pH resulted in bleaching of the visible absorption maxima within 60 min via a two-step reaction with concomitant inactivation of the protein (Wariishi & Gold, 1989, 1990). Photochemical reduction of resting enzyme in the presence of deazoflavin and EDTA followed by oxygenation with O_2 or air or O_2-containing solution also resulted in formation of compound III (H1 or H8), but a Soret absorption maximum of 417 nm was observed (Cai & Tien, 1990), possibly indicating a mixture of forms. The ferrous-oxy form of H8 was very stable at pH 3.5 or 7.0 while the ferrous-oxy form of H1 returned to the resting form with a half-life of 52 min at pH 4.5 and 29 min at pH 7.0. This turnover to resting enzyme was spontaneous and did not require the presence of VA. Although it is not clear how similar the strains and isozymes used in the above studies are, differences in pH and source organism probably explain the various published differences. Most recently, Wariishi and Gold (1990) used three methods to produce lignin peroxidase compound III. Resting enzyme was demonstrated to react with excess H_2O_2 at pH 4.5 to form compound III*. This is the same species described by Renganathan and Gold (1986) and Wariishi et al. (1990) and has the Soret maximum absorbance at 419 nm. Compound III* reacts with catalytic quantities of catalase (also at pH 4.5) to produce compound III-c. Resting enzyme reacted with superoxide anion [produced in situ from the aerobic oxidation of dihydroxyfumarate (DHF) to diketosuccinate] at pH 4.5 to produce compound III-b. Finally, resting enzyme was reduced with 30 equiv of sodium dithionite at pH 4.5 followed by purging with oxygen to produce compound III-a. Compounds III-a, -b, and -c are all characterized by a Soret absorbance at 414 nm. Resonance Raman spectroscopy of all four forms of lignin peroxidase compound III is reported by Mylrajan et al. (1990) and suggests they are all very similar hexacoordinate low-spin forms. The iron–porphyrin vibration analysis suggests that a ferric-superoxide ($Fe^{3+}O_2^{\bullet-}$) structure is most likely. The blue-shift of the Soret region observed in compounds III-a, -b, and -c with respect to compound III* is probably due to an additional molecule of H_2O_2 bound in the pocket of compound III* (Wariishi & Gold, 1990).

Although the lignin peroxidases exhibit reactions that appear typical of other heme-containing peroxidases, they are different in one important respect, namely, the ability to oxidize compounds of high redox potential such as lignin and its model compounds and a variety of xenobiotics. That the iron heme is central to peroxidative chemistry is unequivocal, so a study of the iron and its immediate environment can provide information that is pivotal to our understanding of the structural and mechanistic features that confer these unusual properties on this enzyme. X-ray absorption spectroscopy (XAS) is ideally suited for the investigation of the local environment and electronic structure of the heme iron of hemoproteins. While the edge region of the spectrum provides information about the valence state of the absorbing atom (Fe), the chemically identity of neighboring atoms, and the liganding geometry, the extended X-ray absorption fine structure (EXAFS) region contains information about the number and average distance of ligands and their relative disorder. Not only can differences in Fe–ligand bond lengths be determined to ±0.015 Å but also the relative position of the iron with respect to the heme plane can be investigated (Powers et al., 1981, 1984). Thus, the method offers a sensitive comparison of the active sites of the heme proteins including their reactive intermediates and liganded states (Chance et al., 1984). This work reports the X-ray absorption spectra of the native, reduced, and compound III forms of lignin peroxidase H2 and describes its analysis and significance.

Experimental Procedures

Protein Purification. Lignin peroxidase isoenzyme H2 was purified according to Tuisel et al. (1990); 150-mL cultures were grown in 500-mL Erlenmeyer flasks for 5 days. The extracellular fluid was treated using a freeze/thaw approach to remove mucilaginous material and concentrated prior to FPLC purification of the individual heme-containing fractions. Chromatography was performed using either a Pharmacia Mono Q HR 5/5 column (Pharmacia, Uppsala, Sweden) or a Baker Versa-ten column (J. T. Baker Inc., Phillipsburg, NJ). Peak fractions were dialyzed extensively against water and stored at −20 °C. At this stage, the A_{408}:A_{280} ratio was determined for each preparation and was generally between 4.0 and 4.5.

Preparation of XAS Samples. Intermediate compounds of lignin peroxidase H2 were initially prepared at enzyme concentrations of 10 and 50 μM essentially following the procedures described by Renganathan and Gold (1986) and using an extinction coefficient of 133 mM^{-1} cm^{-1} at 408 nm to determine heme-containing lignin peroxidase concentration.

However, we used 20 mM phosphate buffer at pH 7.0 to maintain consistency with studies on other peroxidases in our laboratory. Resting enzyme had a characteristic Soret absorbance at 408 nm and additional absorbances at 502, 542, and 632 nm. H_2O_2 concentrations were determined by titration with horseradish peroxidase (HRP). At 10 μM, it proved possible to prepare many of the expected intermediates, although compound I was insufficiently stable for further study. Compound I was prepared by titration with a single equivalent of H_2O_2 and was evidenced by a decrease in the Soret absorption. We are not confident that this material was pure and were unable to repeat this study at an enzyme concentration of 50 μM. Compound II was prepared at 10 μM by the addition of 2 equiv of H_2O_2 to resting enzyme and was characterized by the Soret maximum absorbance at 421 nm and the appearance of new absorbance peaks at 531 and 553 nm. Titration with H_2O_2, ascorbic acid, and enzyme revealed the 531:553-nm ratio to be maximal (1.18) with ratios of 1.0:0.5:1.0, which is similar to results we have observed using other peroxidase systems. The conditions used by Renganathan and Gold (1986), involving 2 equiv of H_2O_2 and no ascorbate, also gave acceptable results. Compound II has also been prepared from equimolar amounts of enzyme, H_2O_2, and ferrocyanide (Wariishi & Gold, 1990; Wariishi et al., 1990), but we did not attempt to reproduce these conditions as the presence of additional iron from the ferrocyanide is incompatible with the XAS studies intended for the samples. It was possible to scale these reactions up to 50 μM but not to the millimolar concentrations needed for XAS studies. It is believed that the problem in preparing both compound I and compound II at high concentration lies with the presence of endogenous reductant either as contaminating material in the protein sample or as part of the protein itself (Renganathan & Gold, 1986). Similar problems were encountered during XAS sample preparation of lactoperoxidase intermediates (Chang et al., 1991). Addition of excess H_2O_2 (25 equiv) to resting enzyme (10 μM) produced material having a typical compound III spectrum (Renganathan & Gold, 1986). The Soret maximum is blue-shifted from compound II to 418 nm and the visible peaks red-shifted to 545 and 580 nm. At 200 μM and 2 mM, a 200-fold excess still gave an acceptable compound III spectrum. No bleaching of any absorbances was observed, and the material slowly returned to resting enzyme over some hours. This is consistent with other experiments in progress in our laboratory and with the results of other workers (Wariishi & Gold, 1990; Wariishi et al., 1990) that demonstrate a pH dependence of the turnover of compound III. At 50 μM, the evolution of gas was clearly visible in these experiments, presumed to be oxygen, and indicative of a catalase-like activity. At 1.5 mM, the addition of 25 equiv of H_2O_2 produced a mixture containing some compound III, and 100–200 equiv was generally used. These forms correspond to compound III* (Wariishi & Gold, 1990; Wariishi et al., 1990). Reduced H2 was prepared directly from resting enzyme by the addition of solid sodium dithionite. Its optical spectrum was characterized by a Soret absorbance at 436 nm and a broad visible absorbance containing peaks at 555 and 590 nm. Although we routinely saturate the solutions with nitrogen or argon prior to dithionite addition, this was found to be more important at the lower concentrations, presumably due to the ratio of dissolved O_2 to protein. We also observed the formation of compound III when reduced enzyme was exposed to O_2 and confirm the findings of Wariishi and Gold (1990) and Wariishi et al. (1990) that the Soret absorbance is shifted to 414 nm in this species (referred to in that work as compound III-a). However, the rate of oxygen introduction is not precisely controllable, and we are not able to reproducibly prepare compound III by this means using either lignin peroxidase or a number of other peroxidases. We did not attempt to prepare compound III for XAS studies using this method at higher concentrations.

Protein preparations were concentrated to volumes of approximately 1 mL by ultrafiltration using an Amicon 8010 cell and Amicon Diaflow membranes. If further concentration was necessary, this was achieved by flowing dry nitrogen gas over the surface of the solution at 4 °C. XAS samples generally had protein concentrations of 1.5–2.0 mM. These were prepared in 100 mM phosphate buffer at pH 7.0 and contained 40% ethylene glycol as a cryoprotectant (Chance et al., 1983). Pilot studies were performed to ensure that the cryoprotectant did not alter the optical spectra of the samples or adversely affect the production of intermediates. Following preparation of an intermediate compound at high concentrations, a small aliquot was removed and diluted with buffer to allow optical spectroscopic evaluation of the sample. Although such dilution procedures could possibly provide misleading results, similar methods have been reported for the evaluation of other XAS samples (Chance et al., 1986a,b,c) and are acceptable when the concentrated sample for XAS studies was also monitored by reflectance spectroscopy. The remainder of the sample was immediately loaded into a plexiglass sample holder and frozen in liquid nitrogen. Lignin peroxidase H2 exhibits significant catalatic activity when exposed to high concentrations of H_2O_2 as evidenced by the evolution of gas (presumed to be O_2). With highly concentrated enzyme, the bubbles produced can present problems with homogeneously freezing the samples and scattering problems with the X-ray studies. To eliminate these effects, the reaction mixture was maintained at room temperature until gas evolution had visibly decreased, at which point the sample was briefly centrifuged. This procedure did not noticeably affect the quality of compound III spectra. Reduced enzyme was prepared by adding a small quantity of solid sodium dithionite directly to the sample which had been previously maintained under a nitrogen environment for at least 1 h. A small aliquot of this material was also removed for evaluation by optical techniques and diluted into buffer that had also been saturated with nitrogen.

The quality of XAS samples was carefully monitored throughout the procedure. The veratryl alcohol oxidation activity of the various protein preparations was determined before the final concentration procedures. In addition to the optical spectroscopy described above, reflectance spectroscopy was used to directly examine the visible region of the sample at −100 °C prior to XAS data collection. Samples were stored in liquid nitrogen, and the sample was maintained in a cryostat between −90 and −120 °C during data collection. Following data collection, samples were again stored in liquid nitrogen, and reflectance spectroscopy was repeated before the sample was allowed to thaw. Aliquots of material were then used for dilution and optical absorption analysis, for VA oxidation assay, and for selected SDS–PAGE and/or FPLC analysis. It should be noted here that we do not observe the irreversible inactivation of compound III reported by other investigators. Results obtained in our laboratory and elsewhere (Wariishi & Gold, 1990; Wariishi et al., 1990) suggest that differences in the pH in different studies explain this phenomenon. Incubation of the XAS sample at room temperature for several hours resulted in conversion to a form which had an optical spectrum characteristic of native enzyme, and we were consequently able to fully characterize this material following

X-ray studies. Sample exposure to X-rays was generally between 5 and 10 h.

Data Collection and Analysis. Data collection for lignin peroxidase H2 native and compound III was performed at the National Synchrotron Light Source Beamline X9A (Brookhaven National Laboratory, Upton, NY). The beamline monochromator was equipped with Si 111 crystals, and fluorescence was monitored using a 13-channel germanium detector. H2 native and compound III data collection was repeated at Stanford Synchrotron Light Source beamline 2-1 (Stanford Synchrotron Light Source, Stanford, CA), and the reduced form of H2 was also studied at this time. Si 111 crystals were again employed, but the fluorescence was monitored with a phototube equipped with a phosphorescent screen (Khalid et al., 1986). The EXAFS experimental setup was essentially the same as described previously (Powers et al., 1981), and data having 2–3-eV resolution were collected at 2–4 s per point at energies from 7050 to 7800 eV. Several scans were taken for each sample dependent on both sample concentration and X-ray flux. Data were collected under identical conditions for the model compounds bis(imidazole)(5,10,15,20-tetraphenylporphinato)iron(III) chloride (FeTPP; Collins et al., 1972), ferrous acetylacetonate (Fe^{2+}-acac), and ferric acetylacetonate (Fe^{3+}acac; Iball & Morgan, 1976), except that the transmission mode was used.

Individual spectra were examined for the presence of aberrations, and several were rejected on the grounds of abrupt changes in signal or beam intensity. The remainder were averaged and analyzed by previously reported procedures (Lee et al., 1981; Chance et al., 1984). For samples that were examined at both synchrotron sources, the k^3-multiplied background-subtracted data sets were added together, weighted according to estimates of the signal to noise for each. The edge and ligand field indicator region (LFIR) of each averaged and linear background-subtracted data set was examined (Figure 1). Although the edge region can provide important information about the scatterer, with heme iron the transitions are often too broad to permit rigorous comparisons. However, the ratio of the two LFIR peaks could be easily determined (Chance et al., 1984). The fluorescence amplitude was then normalized to one absorbing atom, multiplied by k^3, and plotted vs k (Figure 2). The different ligand shells were revealed by a Fourier transform of the data shown in Figure 2, as shown in Figure 3. The contribution from the first ligand shell was isolated by a Fourier filter, and the back-transformed data from k = 0–12 Å^{-1} were used for further analysis. Data from 3.5 to 12 Å^{-1} were also examined, and the results were identical. A two-atom fitting procedure (Lee et al., 1981) was used to fit filtered data with FeTPP as a model for Fe–N contributions and Fe^{2+}acac or Fe^{3+}acac as a model for the Fe–O contributions (Powers et al., 1981; Woolery et al., 1985). The numbers of scatterers were constrained to their known values, and 5:1 and 4:2 ratios were respectively used to search parameter space for mathematically and chemically reasonable solutions for axial and Fe–N_p distances, respectively. A three-atom constrained fitting procedure was then used as a consistency test to determine which solutions from the two-atom procedure when combined together were contained in the data. Note that this procedure holds distances (r) and numbers (N) constant so the total number of independent variables is the same as for the two-atom fitting procedure. In order to ensure that this combination was indeed a minimum, each r parameter was separately allowed to vary, holding its corresponding N value and all other r and N values constant. If any r value charged more than the error found from the two-atom-type fitting procedure, the solution was not considered acceptable. The full procedure is described by Chance and co-workers (Chance et al., 1983, 1984). Error estimation was performed as described by Powers and Kincaid (1989). For data extending from k = 0–12 Å^{-1} using a filter of 1.1-Å full-width at half-maximum (Lee et al., 1981), there are 8.4 degrees of freedom in the fit (ϕ_f). Comparison of the fitting results required the sum of the residuals, $\sum R^2 \geq \sum R^2_{min}(1 + 1/\phi_f) \sim \sum R^2_{min}(1.4)$, for two fits to be judged differently. The results for the best solutions in the two-atom fitting procedures and consistency tests for lignin peroxidase H2 native, reduced, and compound III are shown in Table I. The comparison of the residuals from the consistency test with the estimated error is shown in Figure 4 for compound III. These comparisons for native and reduced forms are similar.

Results

Native lignin peroxidase exhibited an absorption spectrum that was very similar to that reported by other groups (Gold et al., 1984; Tien & Kirk, 1984), having a Soret absorption maximum at 408 nm and visible peaks at 505 and 635 nm. Reduced enzyme had a broader Soret absorbance at 436 nm and a broad two-lobed absorbance centered at approximately 550 nm. Compound III made by the addition of excess H_2O_2 exhibited a Soret maximum of 419 nm and visible bands at 546 and 579 nm and corresponds to compound III* described by Wariishi and Gold (1990) and Wariishi et al. (1990). Optical spectra were examined in the reflectance mode before and after data collection, and a small aliquot was thawed, diluted, and immediately examined using transmission after X-ray exposure. No significant degradation of the spectra was observed. Veratryl alcohol oxidation activity was also compared for a small aliquot of sample that was concentrated but not exposed to X-rays with a comparable sample that was exposed to the full duration of X-ray exposure. The native sample retained approximately 80% of its activity, compound III (after turnover to native form) retained approximately 60% of initial activity, and reduced form retained approximately 50% of initial activity. Analytical FPLC was used to further characterize the protein before and after X-ray analysis, and although the reduced form had exhibited some conversion from H2 to H1, a process believed to be due to loss of a phosphate from H2 (Kuan & Tien, 1989), no significant degradation was seen. This was also confirmed by SDS–PAGE, each sample migrating as a single band both before and after X-ray exposure.

The LFIR regions of native lignin peroxidase H2, compound III, and reduced form are shown in Figure 1. The LFIR region of the heme proteins is generally characterized by the ratio of the first peak to the second peak in this part of the spectrum (Chance et al., 1984, 1986a). For native enzyme, this ratio is 1.55 while for compound III and reduced it is 1.06 and 1.07 (±0.05), respectively. Chance et al. (1984) observed that there is a good correlation between the LFIR ratio and the distance by which the iron is displaced from the heme plane, and Chance et al. (1986a) showed this correlation in a number of heme model compounds and used this observation to determine the distance the iron moves during the R- to T-state transition of carp hemoglobin. From this, we can predict that the iron is displaced from the heme plane by 0.6 ± 0.1 Å in native H2 and by 0.3 ± 0.1 Å in both the compound III and reduced forms.

The data plotted as a function of k are shown for the three samples in Figure 2. It can be readily seen that the signal to noise ratio at k = 12 Å^{-1} is sufficiently good to accommodate the subsequent stages of data analysis. A small region

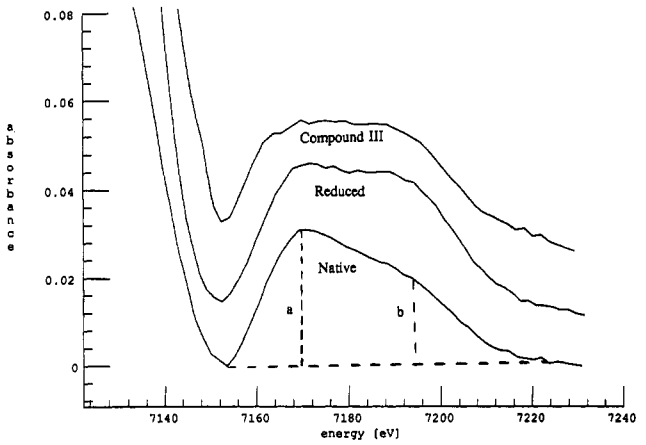

FIGURE 1: LFIR regions of lignin peroxidase H2: native enzyme, compound III, and reduced forms. The LFIR parameter is derived from the ratio of the first to the second peak (*a*:*b*) following linear background subtraction (Chance et al., 1984).

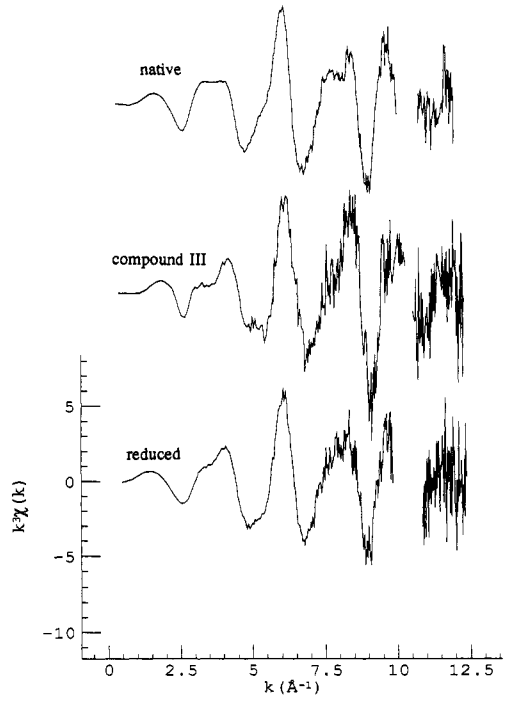

FIGURE 2: Background subtracted data (normalized to one absorbing atom and multiplied by k^3) for lignin peroxidase H2 native enzyme, compound III, and reduced form.

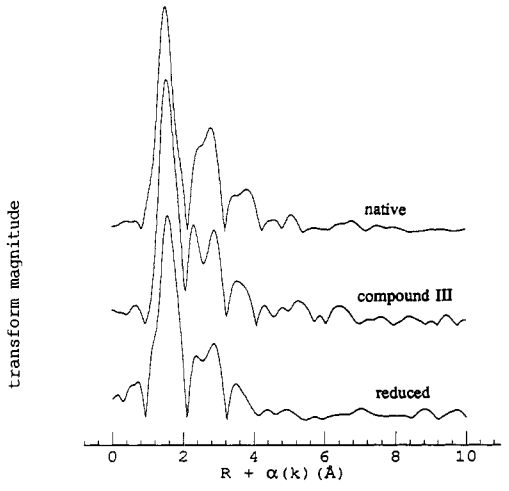

FIGURE 3: Fourier transforms of the EXAFS data in Figure 2 for lignin peroxidase H2 native enzyme, compound III, and reduced form.

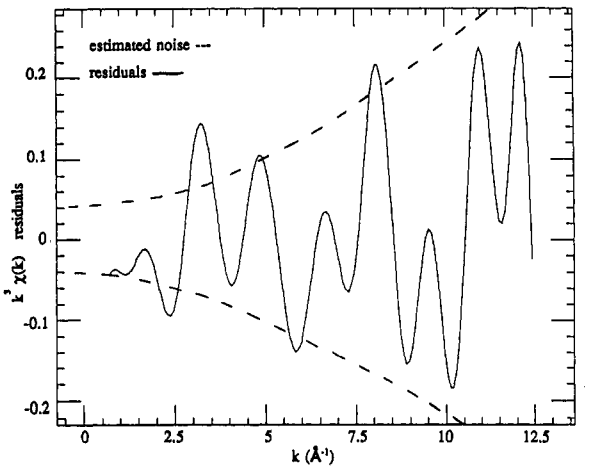

FIGURE 4: Comparison of the residuals for compound III consistency test (Table II) with estimated error. Comparisons for native and reduced forms are similar.

Table I: Fitting Results for the First Coordination Shell of Native Lignin Peroxidase at pH 7[a]

model	N	r	$\Delta\sigma^2$	ΔE_0	$\sum R^2$
Fe–N	4	2.06	2.8×10^{-3}	−0.4	3.7
Fe–N	1	1.92	5.4×10^{-3}	8.0	
Fe–N	5	2.06	1.1×10^{-3}	−0.3	2.7
Fe–N	1	1.92	3.8×10^{-3}	5.8	
Fe–N	5	2.02	1.8×10^{-3}	0.8	5.0
Fe–N	1	2.16	7.5×10^{-3}	4.8	
Fe–N	5	2.07	9.0×10^{-3}	0.8	15.0
Fe–N	1	2.57	-1.4×10^{-2}	−9.2	
Fe–N	4	2.055	2.9×10^{-3}	3.5	1.0
Fe–N	1	1.93	7.0×10^{-3}	−1.7	
Fe–N(O)	1	2.17	-1.5×10^{-3}	−1.5	

[a] $\Delta\sigma^2$ and ΔE_0 are unknown minus model, and N values were held constant. Errors are as follows: Fe–N_p, ±0.015 Å; Fe–N_e, ±0.02 Å; Fe–X, ±0.03 Å; $\Delta\sigma^2$, ±45%; ΔE_0, ±2.5 eV. The consistency test (last entry) has the same degrees of freedom in the fit as the two-atom-type fitting procedures.

Table II: Fitting Results for the First Coordination Shell of Lignin Peroxidase Compound III[a]

model	N	r	$\Delta\sigma^2$	ΔE_0	$\sum R^2$
Fe–N	5	2.03	4.7×10^{-3}	0.0	4.0
Fe–N	1	1.92	9.2×10^{-3}	−5.1	
Fe–N	5	1.99	4.7×10^{-3}	0	4.2
Fe–N	1	2.10	1.0×10^{-2}	6.7	
Fe–N	5	2.03	1.3×10^{-3}	−2.2	6.7
Fe–N	1	1.70	-3.5×10^{-5}	−4.2	
Fe–N	4	2.02	7.1×10^{-3}	0.4	2.2
Fe–N	1	1.90	7.7×10^{-3}	−4.9	
Fe–N(O)	1	1.74	-5.1×10^{-3}	−1.2	
Fe–N	4	1.99	7.1×10^{-3}	3.1	2.4
Fe–N	1	2.09	1.2×10^{-2}	−0.3	
Fe–N(O)	1	1.76	-2.3×10^{-2}	−1.3	
Fe–N	4	1.99	7.2×10^{-3}	0	1.5
Fe–N	1	2.09	1.2×10^{-2}	6.2	
Fe–N(O)	1	1.90	-3.3×10^{-2}	−0.2	

[a] $\Delta\sigma^2$ and ΔE_0 are unknown minus model, and N values were held constant. Errors are as follows: Fe–N_p, ±0.015 Å; Fe–N_e, ± 0.02 Å; Fe–X, ±0.03 Å; $\Delta\sigma^2$, ±45%; ΔE_0, ±2.5 eV. The consistency tests (last three entries) have the same degrees of freedom in the fit as the two-atom-type fitting procedures.

around $k = 10$ Å^{-1} was anomalous due to a multiple reflection from the Si 111 crystals and was removed from the data. It is important to stress that the same anomalous region of the data was also removed from the model compounds (Lee et al., 1981). The Fourier-transformed data are shown in Figure 3 which reveals a well-defined contribution from the first shell of scatterers which was isolated by a Fourier filter and used

Table III: Fitting Results for the First Coordination Shell of Reduced Lignin Peroxidase[a]

model	N	r	$\Delta\sigma^2$	ΔE_0	$\sum R^2$
Fe–N	4	2.04	3.8×10^{-3}	−1.3	3.4
Fe–N	1	1.90	7.0×10^{-3}	2.6	
Fe–N	5	2.04	2.9×10^{-3}	0.4	1.3
Fe–N	1	1.91	6.2×10^{-3}	−2.1	
Fe–N	5	2.01	-3.8×10^{-3}	−0.7	2.3
Fe–N	1	2.11	8.7×10^{-3}	2.4	
Fe–N	5	2.03	-3.5×10^{-3}	−0.5	4.7
Fe–N	1	2.33	7.3×10^{-3}	27.0	
Fe–N	4	2.02	3.5×10^{-3}	−0.3	1.1
Fe–N	1	1.91	5.6×10^{-3}	0.4	
Fe–N(O)	1	2.10	-6.8×10^{-3}	−0.2	

[a] $\Delta\sigma^2$ and ΔE_0 are unknown minus model, and N values were held constant. Errors are as follows: Fe–N_p, ±0.015 Å; Fe–N_e, ±0.02 Å; Fe–X, ±0.03 Å; $\Delta\sigma^2$, ±45%; ΔE_0, ±2.5 eV. The consistency test (last entry) has the same degrees of freedom in the fit as the two-atom-type fitting procedures.

for further analysis. Table I shows the results of both the two-atom fitting procedures and consistency tests for native enzyme, Table II for compound III, and Table III for the reduced forms.

The two-atom fitting procedure for the native enzyme data (Table I) using a 4:1 amplitude ratio revealed four ligands at an average distance of 2.06 Å and one at 1.92 Å (A); 5:1 amplitude ratio fits for the native enzyme suggested axial ligands at 1.92 and 2.16 Å. Although one 5:1 fit gave somewhat improved results over the 4:1 fit, suggesting there to be six ligands in total, the three-atom consistency test (Table I, last entry) demonstrated conclusively that there are in fact six ligands since the $\sum R^2$ decreases by more than a factor of 2. The data can therefore be explained by four ligands at 2.055 ± 0.015 Å, a fifth at 1.93 ± 0.02 Å, and a sixth at 2.17 ± 0.03 Å. Similarly, for the reduced form (Table III), the two-atom fitting procedures suggest the existence of a sixth ligand using 4:1 and 5:1 amplitude ratios. The three-atom consistency test (Table III, last entry) confirmed the existence of a sixth ligand and revealed that four atoms at 2.02 ± 0.015 Å, a fifth at 1.91 ± 0.02 Å, and a sixth at 2.10 ± 0.03 Å were contained within the data. Note that the fourth solution is unacceptable by our criteria due to the large ΔE_0 value. The fitting results for compound III (Table II) are not as well-defined. Unlike the native or reduced forms, three axial distances are found using the 5:1 amplitude fits: 1.92, 2.10, and 1.70 Å. The fact that the two-atom fitting procedures identify three solutions for two distances can occur for two reasons. Either one or more solutions are artifacts of the fitting procedures since three contributions are being averaged as two, or there are actually species with some or all combinations of these axial distances. The three-atom consistency tests have been shown to distinguish fitting procedure artifacts (Chance et al., 1983; Powers et al., 1984) from mixtures (Woolery et al., 1985). The results for the consistency tests for compound III are given as the last three entries in Table II. The first test having four nitrogens at an average distance of 2.02 Å and axial ligands at 1.90 and 1.74 Å also has physically reasonable parameters for $\Delta\sigma^2$ and ΔE_0 (Chance et al., 1983; Powers et al., 1984). The other two tests having combinations of the axial distance solutions have large $\Delta\sigma^2$ parameters for both of the axial solutions. The $\Delta\sigma^2$ parameter describes the change in disorder, both thermal and lattice, between the sample and the model. At room temperature, solution samples have values of $\sigma \sim 10^{-1}$ Å. Thus, $\Delta\sigma^2$ values of -10^{-2} Å^2 are usually considered an upper limit for physically reasonable values (Lee et al., 1981), since σ value for our models are at least an order of magnitude smaller. However, $\Delta\sigma^2$ has an estimated error of 45%, and values of -10^{-2} Å^2 have been reported for many protein samples [for example, see Bunker and Stern (1977), Heald et al. (1979), and Maroney et al. (1989)]. A large positive $\Delta\sigma^2$ value for the other axial ligand in the last two tests of Table II indicates that the distance is less disordered (more ordered) than the model. This appears physically reasonable if the distance is considerably shorter than the model, implying a stronger bond. This is the case for the first consistency test of Table II (1.90- and 1.74-Å axial solutions) and is similar to that of the consistency tests for the native and reduced enzymes (Tables I and III). However, in the other two tests, the positive $\Delta\sigma^2$ value is larger than that of the first test and those of the native and reduced forms while the 2.09-Å axial distance is longer than the model. Although this is physically not impossible, when coupled with the large negative $\Delta\sigma^2$ values of the other axial solution, the last two consistency tests are much less physically reasonable than the first. The most likely explanation for these solutions, on the basis of previous experience with peroxidase samples (Chance et al., 1984, 1986b,c; Chang et al., unpublished results; Woolery et al., 1985), is that the first consistency test represents a large portion of the sample (>85%) and the 2.09-Å axial solution arises from small portions of contaminating species. Various combinations of ligands not shown in the tables were also used to confirm these results and to rule out other possibilities. In addition, the native and compound III data, which were collected at two different synchrotron sources, were each analyzed separately. Lastly, as a final check, the analysis was repeated with data collected for Fe–N and Fe–O model compounds in previous synchrotron runs with identical results.

Table IV: Comparison of LFIR Parameters (±0.05) and Iron Heme Ligand Geometries for Lignin Peroxidase H2 Native Enzyme, Compound III, and Reduced Form[a]

protein	LFIR	Fe–N_p	Fe–Ne	Fe–X(O)
lignin peroxidase				
H2 native (H_2O)	1.55	2.055	1.93	2.17
compound III	1.06	2.02	1.90	1.74
reduced	1.07	2.02	1.91	2.10
horseradish peroxidase				
native	1.33	2.04	1.90	2.39
compound III	1.00	2.02	1.92	1.72
reduced	1.00	2.01	1.90	2.38
myoglobin				
met (H_2O)	1.35	2.04	2.11	1.88
peroxide compound	0.90	1.98	2.11	1.69
oxy	0.93	2.00	2.07	1.83
deoxy	1.33	2.06	2.12	
CN compound	0.68	1.98	2.07	1.86

[a] In addition, comparable data for HRP (Chance et al., 1984, 1986b) and myoglobin (Chance et al., 1983) are shown.

Discussion

The results of the LFIR analysis (Figure 1 and Table IV) show the iron to be significantly out of the heme plane (0.6 Å) in the native enzyme and considerably less so (0.3 Å) in compound III and reduced forms. The phenomenon of the LFIR ratio decreasing as native enzyme is converted to compound III or reduced form has been observed with other peroxidases, notably HRP (Table IV; Chance et al., 1984). It should be noted that the characteristic shape of the LFIR region is a consequence of multiple scattering (Chance et al., 1983). Ruffling of the heme plane could give misleading results, but while we acknowledge that the heme will certainly ruffle to some degree, we do not believe the magnitude of the distortion would be great enough to unduly bias these results. The use of other spectroscopies or different EXAFS analytical techniques can further resolve this question.

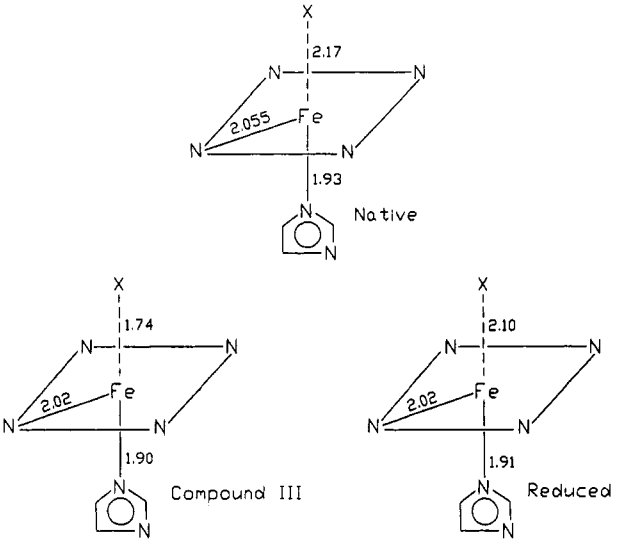

FIGURE 5: Structure of the iron environment of the heme active site of lignin peroxidase H2 native enzyme, compound III, and reduced form is depicted. Distances are in angstroms (Å). Errors are given in the text.

The results of the fitting procedures are shown in Figure 5 and tabulated in Table IV. These reveal that the data for native lignin peroxidase H2 can accommodate four nitrogen atoms at an average distance of 2.055 Å, a fifth (proximal) nitrogen at 1.93 Å, and a sixth (distal) ligand, presumably oxygen, at 2.17 Å. These values are within the error of those we find for the native enzyme at pH 3 (unpublished observations). This result, from data collected at −100 °C, is in agreement with previously published data (Kuila et al., 1985; Andersson et al., 1987) where the iron present in native lignin peroxidase was reported to be a high-spin pentacoordinate system at 25 °C and to change to largely hexacoordinate at significantly lower temperature. Reduced enzyme is also 6-coordinate. The pyrrole nitrogen atoms are located at an average distance of 2.02 Å, the proximal nitrogen at 1.91 Å, and the distal ligand at 2.10 Å. These results are similar to those obtained for HRP (Table IV; Chance et al., 1984b,c). Although the fitting results for compound III were not well-defined, the physically most reasonable solution has the pyrrole nitrogens at an average distance of 2.02 Å, the proximal nitrogen at 1.93 Å, and the distal oxygen at 1.74 Å. From purely physical and mathematical arguments as well as experience, the most likely explanation of the 2.09-Å axial solution was that it arises from small amounts (<15%) of contaminating species. Several other results support this explanation. First, it is difficult to purify peroxidase enzymes without exogenous reductants remaining in the preparation. This further complicates sample preparation which is already difficult at high concentrations. Even though we assessed the purity of the samples at these concentrations, reflectance spectroscopy has much larger error bars than transmission spectroscopy of dilute samples. Furthermore, optical spectroscopy on the diluted samples may not quantitatively represent the concentrated samples at low temperature since the reaction rates depend on temperature and concentration. Even with our careful optical characterization, it is likely that a small amount (<15%) of native enzyme is present in the compound III samples used for XAS measurements. The fact that the axial distance of 2.09 Å is similar to that found as the sixth ligand for the native enzyme further supports this argument. In addition, the most physically reasonable solution is similar to those reported for compounds III of other peroxidases (Table IV; Chance et al., 1984, 1986b,c; Chang et al., unpublished results), as is expected from the similarity of optical spectra and biochemical data. Compound III and reduced forms of both lignin peroxidase and HRP have a more compact average iron–pyrrole nitrogen distance than the native enzyme, which is revealed by both a decrease in the distance by which the iron is out-of-plane (determined from the LFIR) and a corresponding decrease in the iron to pyrrole nitrogen distance contained in the XAS data. Within their respective errors, these results are in agreement with the resonance Raman results of Mylrajan et al. (1990).

Chance et al. (1986b) noted a significant difference between the heme active site of HRP (Chance et al., 1984) and the oxygen transport protein myoglobin. All intermediates of myoglobin were demonstrated to have an iron to proximal histidine nitrogen distance of close to 2.1 Å while the comparable distances in HRP were closer to 1.9 Å (Table IV). The iron to proximal histidine distances for cytochrome *c* peroxidase native (Chance et al., 1984) and compound ES (Chance et al., 1986a) were also demonstrated to be 1.94 and 1.91 Å, respectively, suggesting that a general structural difference between the oxygen transport proteins and the peroxidases might be revealed by the distance from the iron to proximal histidine nitrogen. That the iron to histidine nitrogen distance determined by XAS spectroscopy is longer in the oxygen transport proteins than in the peroxidases is additionally supported by recent high-resolution crystal structures of various myoglobins (horse heart metmyoglobin, 2.23 Å; Evans & Breyer, 1990; ferric sperm whale myoglobin–imidazole complex, 2.04 Å; Lionetti et al., 1991). The heme active-site structure of lignin peroxidase is also in good agreement with this trend, having an iron to proximal histidine distance of 1.93 Å in the native enzyme and 1.91 Å in both compound III and reduced enzyme. Several experiments on other proteins, such as lactoperoxidase (Chang et al., unpublished results), currently in progress in our laboratory, confirm that this structural feature appears to be generally applicable to the heme peroxidases.

Another emerging trend concerns the relative expansion of the average heme iron–pyrrole nitrogen distance in the different peroxidases. The distance by which the iron is displaced from the heme plane is one indicator of this structural feature. That the lignin peroxidases are considerably more potent oxidants than HRP is clearly evidenced by the ability of the white rot fungus to degrade a number of persistent xenobiotic compounds (Bumpus et al., 1985; Bumpus & Aust, 1987a,b; Eaton, 1985; Arjmand & Sanderman, 1985; Bumpus & Brock, 1988; Mileski et al., 1988; Valli & Gold, 1991) and by the demonstration that purified lignin peroxidase protein is directly implicated in at least the initial stages of this mineralization process (Bumpus & Brock, 1988; Mileski et al., 1988; Sanglard et al., 1986; Haemmerli et al., 1986; Hammel et al., 1986, 1988; Screiner et al., 1988; Valli & Gold, 1991). Many of these compounds have extremely high redox potentials (Hammel et al., 1986; Kersten et al., 1985; Kamaya & Higuchi, 1984) and are consequently completely resistant to degradation by HRP and other peroxidases. It is therefore tempting to pose the hypothesis that the reactivity of the peroxidases is correlated to the relative expansion of the average heme iron–pyrrole nitrogen distance in just the opposite way to that observed in the oxygen transport proteins. In hemoglobin and myoglobin, a contracted heme (R state) is correlated with higher reactivity than an expanded heme (T state), while in the peroxidases, if lignin peroxidase is a typical example of the trend, increased reactivity seems to be correlated with an expanded heme. We are studying a number of

different peroxidases in our laboratory, and it should be noted that lignin peroxidase H2 exhibits the most expanded heme iron–pyrrole nitrogen distance observed to date.

Millis et al. (1989) performed electrochemical studies to determine the oxidation–reduction potential of ferrous/ferric lignin peroxidase. The conclusions from that work were that lignin peroxidase has a more electron-deficient heme environment than other peroxidases. This was correlated with the oxidation–reduction potentials of HRP compounds I and II (Hayashi & Yamazaki, 1979) and with the estimation of the redox potential of the lignin peroxidase from their ability to oxidize various substrates (Hammel et al., 1986). It seems possible that the reported electron deficiency is a more localized consequence of redistribution of the heme electrons. An expanded heme, due to a longer average iron–pyrrole nitrogen distance, might be anticipated to possess such an altered electron distribution. The same porphyrin structure is present in both the oxygen transport proteins and the peroxidases and furthermore, in all cases, is linked to the protein via a single histidine nitrogen. It is clear that structural features in the protein portion of these molecules play an important role in the structural changes we are able to measure in the heme, but to date, the nature of these protein-based components remains unclear. Comparison of the cDNA sequences of the lignin peroxidases with other heme proteins reveals that the distal histidine, conserved in other heme proteins, is also present in the lignin peroxidases (Tien & Tu, 1987a,b; deBoer et al., 1987; Zhang et al., 1991) and, additionally, residues flanking this histidine are also conserved. Poulos and Kraut (1980) propose that in cytochrome *c* peroxidase (CcP) this histidine is responsible for the ionization that controls the reaction of native enzyme with H_2O_2, the acidic form being less reactive. However, compound I formation shows no pH dependence in the acidic range for the lignin peroxidases (Welinder, 1979; Tien et al., 1986), which suggests that mechanism may not apply in this case. It has been demonstrated that an aspartate residue (Asp-235) controls the rate of reaction with hydrogen peroxide in CcP (Edwards et al., 1984; Loo & Erman, 1975) and therefore the pH dependence of compound I formation might also be dependent on protonation of this group. This would correspond to Asp-43 of HRP (Welinder, 1979) and Asp-48 of lignin peroxidase (Tien & Tu, 1987a,b). An aspartate located close to a positive charge could have a pK_a as low as 2.0 which would be consistent with the extremely low pH optimum described for lignin peroxidases (Andrawis et al., 1988; Tien et al., 1986), although the precise differences between lignin peroxidase and HRP in this respect are not understood. The differences between lignin peroxidase and other peroxidases still remain to be determined, and although there is substantial evidence that hydrogen bonding of the N_d atom of the proximal histidine influences imidazole basicity which in turn affects the oxidation–reduction potential of the heme (Poulos & Kraut, 1980; Takano, 1977a,b; Terakoka & Kitagawa, 1981; deRopp et al., 1985, LaMar, 1982), exact correlations between these structural features and the reactivities of the oxygen carriers and peroxidases are still lacking.

We have determined the heme iron geometry of lignin peroxidase H2, native enzyme, compound III, and reduced enzyme and have shown that, like other peroxidases, these species have a shorter iron to proximal histidine nitrogen distance than the oxygen carriers. In addition, we have shown that the higher redox potential of the lignin peroxidases appears to be correlated with a more expanded average iron to pyrrole nitrogen distance, lignin peroxidase exhibiting the most expanded heme we have observed among several peroxidases. Although X-ray crystal structures are available for both myoglobin and CcP, preliminary data are available for HRP (Morita et al., 1990), and successful crystallization of lignin peroxidase has been demonstrated (Troller et al., 1988), more structures are needed before critical regions close to the heme that affect its structure can be assessed.

ACKNOWLEDGMENTS

We thank the National Bio-structures Participating Research Team for allocation of beam time and for experimental support on X-9 at the National Synchrotron Light Source, Brookhaven National Laboratory, Upton, NY, and Dr. S. M. Khalid for assistance in data collection there and also at the Stanford Synchrotron Radiation Laboratory, Stanford Linear Accelerator Center, Stanford, CA, where part of this work was performed under Proposal 2060. We are grateful to Dr. Mike Gold for valuable discussions and critical reading of the manuscript.

REFERENCES

Andersson, L. A., Renganathan, V., Chiu, A. A., Loehr, T. M., & Gold, M. H. (1985) *J. Biol. Chem. 260*, 6080–6087.
Andersson, L. A., Renganathan, V., Loehr, T. M., & Gold, M. H. (1987) *Biochemistry 26*, 2258–2263.
Andrawis, A., Johnson, K. A., & Tien, M. (1988) *J. Biol. Chem. 263*, 1195–1198.
Arjmand, M., & Sanderman, H. (1985) *J. Agric. Food Chem. 33*, 1055–1060.
Bumpus, J. A., & Aust, S. D. (1987a) *BioEssays 6*, 166–170.
Bumpus, J. A., & Aust, S. D. (1987b) *Appl. Environ. Microbiol. 53*, 2001–2008.
Bumpus, J. A., & Brock, B. J. (1988) *Appl. Environ. Microbiol. 54*, 1143–1150.
Bumpus, J. A., Tien, M., Wright, D., & Aust, S. D. (1985) *Science 228*, 1434–1436.
Bunker, B., & Stern, E. (1977) *Biophys. J. 19*, 253–264.
Cai, D., & Tien, M. (1990) *Biochemistry 29*, 2085–2091.
Chance, B., Fischetti, R., & Powers, L. (1983) *Biochemistry 22*, 3820–3829.
Chance, B., Powers, L., Ching, Y., Poulos, T., Yamazaki, I., & Paul, K. G. (1984) *Arch. Biochem. Biophys. 235*, 596–611.
Chance, M., Parkhurst, L. J., Powers, L. S., & Chance, B. (1986a) *J. Biol. Chem. 261*, 5689–5692.
Chance, M., Powers, L., Kumar, C., & Chance, B. (1986b) *Biochemistry 25*, 1259–1265.
Chance, M., Powers, L., Poulos, T., & Chance, B. (1986c) *Biochemistry 25*, 1266–1270.
Collins, D., Countryman, R., & Hoard, J. (1972) *J. Am. Chem. Soc. 94*, 2066–2072.
deBoer, H. A., Zhang, Y. Z., Collins, E., & Reddy, E. A. (1987) *Gene 60*, 93–102.
deRopp, J. S., Thanabal, V., & LaMar, G. N. (1985) *J. Am. Chem. Soc. 107*, 8268–8270.
Dunford, H. B. (1982) *Adv. Inorg. Biochem. 4*, 41–68.
Dunford, H. B., & Stillman, J. S. (1976) *Coord. Chem. Rev. 19*, 187–251.
Eaton, D. C. (1985) *Enzyme Microb. Technol. 7*, 194–196.
Edwards, S. L., Poulos, T. L., & Kraut, J. (1984) *J. Biol. Chem. 259*, 12984–12988.
Evans, S., & Breyer, G. (1990) *J. Mol. Biol. 213*, 885–897.
Farrell, R. L., Murtagh, K. E., Tien, M., Mozuch, M. P., & Kirk, T. K. (1989) *Enzyme Microb. Technol. 11*, 322–328.
Godfrey, B. J., Mayfield, M. B., Brown, J. A., & Gold, M. H. (1990) *Gene 93*, 119–124.

Gold, M. H., Wariishi, H., & Valli, K. (1979) *ACS Symp. Ser. 389*, 127–140.
Gold, M. H., Kuwahara, M., Chiu, A. A., & Glenn, J. K. (1984) *Arch. Biochem. Biophys. 234*, 353–362.
Haemmerli, S. D., Leisola, M. S. A., Sanglard, D., & Fiechter, A. (1986) *J. Biol. Chem. 261*, 6900–6903.
Hammel, K. E., & Tardane, P. J. (1988) *Biochemistry 27*, 6563–6568.
Hammel, K. E., Kalyanaraman, B., & Kirk, T. K. (1986) *J. Biol. Chem. 261*, 16948–16952.
Hayashi, Y., & Yamazaki, I. (1979) *J. Biol. Chem. 254*, 9101–9106.
Heald, S., Stern, E., Bunker, B., Holt, E., & Holt, S. (1979) *J. Am. Chem. Soc. 101*, 67–73.
Iball, J., & Morgan, C. (1976) *Acta Crystallogr., Sect. B B23*, 239–244.
Jeffries, T. W., Choi, S., & Kirk, T. K. (1981) *Appl. Environ. Microb. 42*, 290–296.
Kamaya, T., & Higuchi, T. (1984) *FEMS Microbiol. Lett. 22*, 89–92.
Kersten, P. J., Tien, M., Kalyanaraman, B., & Kirk, T. K. (1985) *J. Biol. Chem. 260*, 2609–2612.
Keyser, P., Kirk, T. K., & Zeikus, J. G. (1978) *J. Bacteriol. 73*, 294–306.
Khalid, S., Rosenbaum, G., & Chance, B. (1986) *Proc. SPIE—Int. Soc. Opt. Eng. 690*, 65–67.
Kirk, T. K., Croan, S., Tien, M., Murtagh, K. E., & Farrell, R. L. (1986) *Enzyme Microb. Technol. 8*, 27–32.
Kohler, A., Jager, A., Willershausen, H., & Graf, H. (1988) *Appl. Microbiol. Biotechnol. 29*, 618–620.
Kuan, I.-C., & Tien, M. (1989) *J. Biol. Chem. 264*, 350–355.
Kuila, D., Tien, M., Fee, J. A., & Ondrias, M. R. (1985) *Biochemistry 24*, 3394–3397.
LaMar, G. N., & de Ropp, J. S. (1982) *J. Am. Chem. Soc. 104*, 5203–5206.
Lee, P., Citrin, P., Eisenberger, P., & Kincaid, B. (1981) *Rev. Mod. Phys. 53*, 769–806.
Leisola, M. S. A., Kozulic, B., Meusdoerffer, F., & Fiechter, A. (1987) *J. Biol. Chem. 262*, 419–424.
Lionetti, C., Guanziroli, M., Frigerio, F., Ascenzi, P., & Bolognesi, M. (1991) *J. Mol. Biol. 217*, 409–412.
Loo, S., & Erman, J. E. (1975) *Biochemistry 14*, 3467–3470.
Maroney, M., Scarrow, R., Que, L., Jr., Roe, A., Lukat, G., & Kurtz, D. (1989) *Inorg. Chem. 28*, 1342–1348.
Marquez, L., Wariishi, H., Dunford, H. B., & Gold, M. H. (1988) *J. Biol. Chem. 263*, 10549–10552.
Mileski, G. J., Bumpus, J. A., Jurek, M. A., & Aust, S. D. (1988) *Appl. Environ. Microbiol. 54*, 2885–2889.
Millis, C. D., Cai, D., Stankovich, M. T., & Tien, M. (1989) *Biochemistry 28*, 8484–8489.
Morita, Y., Mikami, B., Yamashita, H., Lee, J. Y., Sato, M., Katsube, Y., & Tanaka, N. Abstract for the Peroxidase Symposium, Aug 27–29, 1990, Lublin, Poland.
Mylrajan, M., Valli, K., Wariishi, H., Gold, M. H., & Loehr, T. M. (1990) *Biochemistry 29*, 9617–9623.
Poulos, T. L., & Kraut, J. (1980) *J. Biol. Chem. 255*, 8199–8205.
Powers, L., & Kincaid, B. (1989) *Biochemistry 28*, 4461–4468.
Powers, L., Chance, B., Ching, Y., & Angiolillo, P. (1981) *Biophys. J. 34*, 465–498.
Powers, L., Sessler, J., Woolery, G., & Chance, B. (1984) *Biochemistry 23*, 239–244.
Pribnow, D., Mayfield, M. B., Nipper, V. J., Brown, J. A., & Gold, M. H. (1989) *J. Biol. Chem. 264*, 5036–5040.
Renganathan, V., & Gold, M. H. (1986) *Biochemistry 25*, 1626–1631.
Sanglard, D., Leisola, M. S. A., & Fiechter, A. (1986) *Enzyme Microb. Technol. 8*, 209–212.
Sarkanen, S., Razal, R. A., Piccariello, T., Yamamoto, E., & Lewis, N. G. (1991) *J. Biol. Chem. 266*, 3636–3643.
Schreiner, R. P., Stevens, J. E., & Tien, M. (1988) *Appl. Envirol. Microbiol. 54*, 1858–1860.
Smith, T. L., Schlach, H., Gaskell, J., Covert, S., & Cullen, D. (1988) *Nucleic Acids Res. 16*, 1219.
Takano, T. (1977a) *J. Mol. Biol. 110*, 537–568.
Takano, T. (1977b) *J. Mol. Biol. 110*, 569–584.
Teraoka, J., & Kitagawa, T. (1981) *J. Biol. Chem. 256*, 3969–3977.
Tien, M. (1987) *Crit. Rev. Microbiol. 13*, 141–168.
Tien, M., & Kirk, T. K. (1984) *Proc. Natl. Acad. Sci. U.S.A. 81*, 2280–2284.
Tien, M., & Tu, C.-P. D. (1987) *Nature 326*, 520–523.
Tien, M., & Tu, C.-P. D. (1987b) *Nature 328*, 742.
Tien, M. Kirk, T. K., Bull, C., & Fee, J. A. (1986) *J. Biol. Chem. 261*, 1687–1693.
Troller, J., Smit, J. D. G., Leisola, M. S. A., Kallen, J., Winterhalter, K. H., & Fiechter, A. (1988) *Bio Technology 6*, 571–573.
Tuisel, H., Sinclair, R., Bumpus, J. A., & Aust, S. D. (1990) *Arch. Biochem. Biophys. 279*, 158–166.
Valli, K., & Gold, M. H. (1991) *J. Bacteriol. 173*, 345–352.
Wariishi, H., & Gold, M. H. (1989) *FEBS Lett. 243*, 165–168.
Wariishi, H., & Gold, M. H. (1990) *J. Biol. Chem. 265*, 2070–2077.
Wariishi, H., Marquez, L., Dunford, H. B., & Gold, M. H. (1990) *J. Biol. Chem. 265*, 11137–11142.
Welinder, K. G. (1979) *Eur. J. Biochem. 96*, 483–502.
Woolery, G., Walters, M., Suslick, K., Powers, L., & Spiro, T. (1985) *J. Am. Chem. Soc. 107*, 2370–2373.
Yamazaki, I. (1974) in *Molecular Mechanisms and Oxygen Activation* (Hayaishi, O., Ed.) pp 535–559, Academic Press, New York.
Zhang, Y. Z., Reddy, C. A., & Rasooly, A. (1991) *Gene 97*, 191–198.